



Published in final edited form as:

Inflamm Bowel Dis. 2012 January ; 18(1): 101–111. doi:10.1002/ibd.21744.

Loss of Downregulated in Adenoma (DRA) Impairs Mucosal HCO_3^- Secretion in Murine Ileocolonic Inflammation

Fang Xiao*, Marina Juric*, Junhua Li*,[¶], Brigitte Riederer*, Sunil Yeruva*, Anurag Kumar Singh*, Lifei Zheng*,^{**}, Silke Glage[†], George Kollias[‡], Pradeep Dudeja[§], De-An Tian^{||}, Gang Xu[¶], Jinxia Zhu^{**}, Oliver Bachmann*, and Ursula Seidler*

*Department of Gastroenterology, Hannover Medical School, Hannover, Germany

[†]Institute of Laboratory Animal Science, Hannover Medical School, Hannover, Germany

[‡]Biomedical Sciences Research Center Alexander Fleming, Greece

[§]Department of Medicine, University of Illinois, Champaign, Illinois

^{||}Department of Gastroenterology, Tongji Hospital, Huazhong University of Science & Technology, China

[¶]Department of Nephrology, Tongji Hospital, Huazhong University of Science & Technology, China

^{**}Department of Physiology, Capital Medical University, China

Abstract

Background—Ileocolonic luminal pH has been reported to be abnormally low in inflammatory bowel disease (IBD) patients, and one of the causative factors may be reduced epithelial HCO_3^- secretory rate ($J_{\text{HCO}_3^-}$). Disturbances in $J_{\text{HCO}_3^-}$ may occur due to inflammation-induced changes in the crypt and villous architecture, or due to the effect of proinflammatory cytokines on epithelial ion transporters.

Methods—To discriminate between these possibilities, the tumor necrosis factor alpha (TNF- α) overexpressing (TNF^{+/ARE}) mouse model was chosen, which displays high proinflammatory cytokine levels in both ileum and colon, but develops only mild colonic histopathology and diarrhea. HCO_3^- secretion, mRNA expression, immunohistochemistry, and fluid absorptive capacity were measured in ileal and mid-colonic mucosa of TNF^{+/ARE} and wildtype (WT) (TNF^{+/+}) mice in Ussing chambers, and in anesthetized mice in vivo.

Results—The high basal $J_{\text{HCO}_3^-}$ observed in WT ileal and mid-colonic mucosa were luminal Cl^- -dependent and strongly decreased in TNF^{+/ARE} mice. Downregulated in adenoma (DRA) mRNA and protein expression was strongly decreased in TNF^{+/ARE} ileocolon, whereas cystic fibrosis transmembrane conductance regulator (CFTR), Na^+/H^+ exchanger 3 (NHE3),

Reprints: Prof. Dr. med. Ursula Seidler, Hannover Medical School, Department of Gastroenterology, Carl-Neuberg-Str. 1, 30625, Hannover, Germany (seidler.ursula@mh-hannover.de).

The first two authors share the first, and the last two share the corresponding authorship.

Permanent address for Fang Xiao: Dept. of Gastroenterology, Tongji Hospital, Huazhong University of Science & Technology, Wuhan, Hubei, China.

Additional Supporting Information may be found in the online version of this article.

$\text{Na}^+/\text{HCO}_3^-$ cotransporter (NBC), and epithelial sodium channel (ENaC) expression was not significantly altered. This indicates that the severe defect in ileocolonic $\text{J}_{\text{HCO}_3^-}$ was due to DRA downregulation. Fluid absorption was severely depressed in the ileum but only mildly affected in the mid-distal colon, preventing the development of overt diarrhea.

Conclusions—Even mild ileocolonic inflammation may result in a decrease of epithelial HCO_3^- secretion, which may contribute to alterations in surface pH, intestinal flora, and mucus barrier properties.

Keywords

inflammatory bowel disease; bicarbonate; anion exchanger; colon

Diarrhea is among the predominant clinical symptoms in inflammatory bowel disease (IBD), and the molecular mechanisms of its origin have been studied for some time.^{1,2} The major electrolyte transporters studied in this respect are the Na^+ -absorptive transporters, the Na^+/H^+ exchanger NHE3, and the epithelial Na^+ channel ENaC.^{3,4} Disturbances in their expression and/or function have been reported in response to the application of tumor necrosis factor alpha (TNF- α) alone or in combination with interferon gamma (IFN- γ) in cell culture,^{5,6} isolated colonic mucosa,⁷ or in vivo.⁸

In a previous study in biopsies from patients with moderately severe ulcerative colitis (UC), we observed a moderate dysfunction of the sodium absorptive exchanger NHE3, but a major decrease of the $\text{Cl}^-/\text{HCO}_3^-$ exchange in the luminal membrane, associated with a downregulation of the anion exchanger DRA (SLC26a3).⁹ DRA is both involved in duodenal HCO_3^- secretion as well as, coupled with NHE3, in jejunal NaCl absorption.^{10,11} Observational and experimental studies have implicated DRA expression as one potential target during intestinal inflammation,^{12,13} but the functional consequences have not been studied.

To learn more about the molecular details and the functional outcome of inflammation-associated changes in epithelial HCO_3^- transport, we selected the TNF^{ARE} mouse model, which in the heterozygous state represents a chronic mild to moderately severe ileocolitis model with high mucosal proinflammatory cytokine levels (higher than in interleukin [IL]-10 KO colitis, transfer colitis, dextran sodium sulfate [DSS]-colitis, and in IBD patient biopsies measured in our laboratory) both in the ileum and colon, but only mild histopathological changes in the colon, and no ulcerations (which would make the study of epithelial ion transport uninterpretable). We characterized epithelial HCO_3^- secretion, fluid absorption, ENaC activity, DRA mRNA and protein in the ileum, and colon TNF^{+/-} ARE and TNF^{+/+} mice. The results suggest that DRA downregulation may be an early event in ileocolonic inflammation, and may be associated with a selective disturbance of epithelial HCO_3^- secretion even before the onset of overt diarrhea.

Materials and Methods

Animals

TNF^{+/ARE} mice, established in the laboratory of Georgios Kollias, were used as a chronic mild/moderate ileocolitis model.¹⁴ Important for our selection of the colitis model was the expression of high mucosal Th1 cytokine levels, the absence of epithelial ulcerations, and no major colonic shortening within the age span of our experiments. The mice were age- and sex-matched, and used in full adulthood, between 3–6 months of age. Mice were sacrificed by CO₂ inhalation followed by cervical dislocation. All experiments were approved by the local Institutional Animal Care and Research Advisory Committee and authorized by the district authority of Hannover.

Histological Scoring

Full-length intestines were excised and fixed in the “swiss roll” technique. Sections of the paraffin-embedded material were made longitudinally, so that the whole length of the ileocolon was visualized. Serial sections were cut and stained with hematoxylin and eosin. The whole length of the ileocolon was assessed with a modified TJL-scoring system.¹⁵ Histological scores were assigned by experimenters “blinded” to sample identity. Distal ileum and mid-colonic inflammation scores were designed separately for severity (S): 0 = normal, 1 = mild (small, focal, or widely separated, limited to lamina propria), 2 = moderate (multifocal or extending to submucosa), 3 = severe (ulcers covering large areas of mucosa); Ulceration (U): 0 = no ulcer, 1 = 1–2 ulcers involving up to 20 crypts, 2 = 1–4 ulcers involving up to 40 crypts, 3 = any group exceeding the above; Hyperplasia (H): 0 = normal, 1 = mild, 2 = moderate, 3 = severe; Area involved (A): 0 = 0%, 1 = 10%–30%, 2 = 40%–70%, 3 = > 70%. Scores for severity, ulceration, hyperplasia, and area involved were added, resulting in a total scoring range of 0–12. Epithelial surface measurements in the ileum and mid-colon are described in the Supplementary Methods.

pH-Stat Titration of J_{HCO₃⁻} in Isolated Distal Ileal, Proximal, and Mid-colonic Mucosa

Ussing chamber experiments were performed as described previously,¹⁶ but were performed in the open circuit mode, with intermittent current pulses (100 μ Amp every 60 sec) to record the electrical resistance and calculate a nominal short circuit current (I_{sc}). The studied segments were: the last 4 cm of ileum, the proximal colon (starting \approx 0.5 cm after the cecocolonic curvature, ending \approx 2 cm after the cecocolonic curvature) and the mid-colon (starting \approx 2 cm after the cecocolonic curvature, ending \approx 4 cm away from the anus). The excised distal ileum, proximal, and mid-colon was stripped of external muscle layers and mounted on Ussing chambers (0.625 cm² aperture). Neural activity and prostaglandin generation were blocked with tetrodotoxin (1 μ M, serosal) and indomethacin (3 μ M, serosal). Transepithelial I_{sc} was calculated as [μ Eq/cm² tissue surface area/h].

The serosal solution contained (in mM): 108 NaCl, 25 NaHCO₃, 3 KCl, 1.3 MgSO₄, 2 CaCl₂, 2.25 KH₂PO₄, 8.9 glucose, and 10 sodium pyruvate, and was gassed with 95% O₂ / 5% CO₂ (pH 7.4). The mucosal solution (154 mM NaCl or 154 mM Na-gluconate) was gassed with 100% O₂. Basal parameters were first measured under a luminal Cl⁻ present condition (i.e., 154 mM NaCl) for 20 minutes, then luminal Cl⁻ was removed by replacing

luminal NaCl with isotonic Na-gluconate solution and the basal bicarbonate secretory rate under Cl^- free condition (i.e., 154 mM Na-gluconate) was measured for 20 minutes. Forskolin was then added to serosal solution with an end concentration of 10 μM and HCO_3^- output was observed for another 30 minutes. HCO_3^- secretory rates were recorded at 2-minute intervals.

I_{sc} Measurements in Voltage Clamp Mode for ENaC Assessment in Distal Colonic Mucosa

For ENaC activity measurements, distal colonic mucosa (the last 1 cm of colon) was studied under voltage clamp conditions with identical electrolyte concentrations in the luminal and the serosal bath, except for 8.9 mM glucose in the luminal and 8.9 mM mannitol in the serosal bath. To assess ENaC current, 10^{-5} M amiloride was added to the luminal bath and the ensuing decrease in current was recorded.

HCO_3^- Secretion and Fluid Absorption in the Ileum and Colon of $\text{TNF}^{+/ \text{ARE}}$ and $\text{TNF}^{+/+}$ Mice

The measurement of HCO_3^- secretion and fluid absorptive rates were performed by single-pass perfusion, as described by us for the duodenum¹⁷ and jejunum,¹⁸ with modifications for the anesthesia as described for the duodenum.¹⁹ For the ileum, the inlet tube was inserted 5 cm proximal to the ileocecal junction and the outlet tube was inserted through the cecum and secured directly at the ileocecal junction; the perfusion rate was 3 mL/h for the experiments in which fluid absorption was measured and 12 mL/h for the HCO_3^- secretory experiments, as described.¹⁷ Because the mouse proximal colon and distal colon are relatively short (about 1–1.5 cm in length respectively) and the in vivo perfusion experiment requires a relatively longer segment (minimum 4–5 cm) to possibly prevent colonic dilatation and gain stable fluid absorptive and luminal alkalinization rates, we divided the colon into two parts for the in vivo perfusion experiments performed, i.e., the proximal mid-colon and mid-distal colon. For perfusing the mid-distal colon, the inlet tube was inserted into the cecum and advanced into the proximal colon and ligated ≈ 1.5 cm after the cecocolonic junction. The outlet tube was inserted through the rectum and fixed at the anal canal. A perfusion speed of 30 mL/h was chosen for the fluid absorptive measurements; to prevent clogging of mucous material, the fluid was recirculated with a precision pump (Gilson minipuls evolution, Villiers, France) and kept at 37°C. For HCO_3^- secretion, identical conditions as for the ileum were chosen. To measure proximal-mid-colonic HCO_3^- secretion, the proximal ligature was placed at the cecocolonic junction and the distal ligature ≈ 3 cm distally. The amount of fluid absorption was assessed gravimetrically and HCO_3^- secretion was determined by pH-stat titration, as described.²⁰ At least two 10-minute collection periods were chosen to ascertain that the secreted HCO_3^- had permeated the mucus and was titrated in the effluent.

Quantitative Polymerase Chain Reaction (PCR) Protocol

RNA was isolated from ileal and colonic tissue of $\text{TNF}^{+/ \text{ARE}}$ and $\text{TNF}^{+/+}$ mice using NucleoSpin RNAII Total RNA Isolation kit (Macherey & Nagel). Reverse transcription was performed with SuperScript III Reverse Transcriptase (Invitrogen, La Jolla, CA). PCR primers were designed using the computer program “Primer Express” (Applied Biosystems, Foster City, CCA) and are shown in Supplementary Table 1. Real-time PCR reactions were carried out using MESA GREEN qPCR Master Mix (Eurogentec) in the Applied

Biosystems 7300 Real-time PCR System as described elsewhere.²¹ PCR extension was performed at 60°C with 40 repeats. Data were analyzed using Sequence Detection Software 1.2.3 (Applied Biosystems) and exported to Microsoft Excel. Relative quantification was carried out using the epithelial specific genes villin and cytokeratin 18, as well as the marker genes RPS9 and actin for total RNA content.

DRA Immunohistochemistry and Confocal Microscopy

Mid-colon freshly taken out from DRA^{-/-} and DRA^{+/+}, TNF^{+/-} ARE, and TNF^{+/+} mice ($n = 3$) was rinsed with ice-cold phosphate-buffered saline (PBS) and fixed for 2 hours at 4°C with 2% paraformaldehyde in PBS. Fixed tissue was rinsed with PBS and transferred to 30% sucrose in PBS overnight. Then the tissue was embedded with tissue-freezing medium (TissueTec O.C.T., Sakura Fine Tek, Torrance, CA). Cryosectioning was done with a microtome cryostat at -20°C. Seven- μ m-thick sections were collected on microscope slides (SuperFrost Plus, Menzel-Gläser, Germany), fixed with 80% acetone for 3 minutes, air-dried, and stored at -20°C. Fixed sections were washed in PBS and blocked with 5% normal goat serum (NGS) for 2 hours. Tissues were then incubated with anti-DRA antibody (1:100) in PBS with 1% NGS for 2 hours at room temperature as described in Gill et al.²² After washing, sections were incubated with Alexa Fluor 488-conjugated goat antirabbit IgG for 60 minutes. The tissues were covered using slow fade with DAPI (Molecular Probes, Invitrogen) which stained the nuclei while mounting. Cover slides were imaged on the confocal microscope with sequential scan imaging (A Leica DM IRB with a TCS SP2 AOBS scan head equipped with a 405 nm laser for excitation of blue dyes).

Agents

Tetrodotoxin was purchased from Biotrend Chemicals (Wengen, Switzerland). Forskolin was purchased from Alexis Biochemicals (Lörrach, Germany). Other reagents were purchased from Sigma-Aldrich (Deisenhofen, Germany).

Statistics

All results are expressed as the mean \pm SE. The data were analyzed by analysis of variance (ANOVA) for multiple comparisons or Student's *t*-tests for paired samples, $P < 0.05$ was considered statistically significant.

Results

Characterization of Ileocolonic Inflammation

For the TNF^{+/-} ARE and TNF^{+/+} mice, an inflammation score with a maximum number of 12 was used to grade the tissues. The TNF^{+/-} ARE tissues had mild/moderate ileal (inflammation score of 4) and milder colonic (inflammation score of 2.5) inflammation, and no inflammation in the TNF^{+/+} ileocolon. Furthermore, the mRNA expression levels of TNF- α , IL-1 β , and IFN- γ were strongly elevated in the ileal as well as the mid-distal colonic tissue of TNF^{+/-} ARE mice compared to WT littermates (Fig. 1A). Histological evaluation confirmed the inflammatory phenotype in all parts of the ileocolon, with subepithelial leukocyte inflammation, marked villus thickening in the ileum, and mild epithelial hypertrophy in the mid-distal colon (Fig. 1B,C). Epithelial surface measurements yielded a

significant reduction of the mucosal surface of approximately half in the ileum, but not in the mid-colon.

Characterization of HCO_3^- Secretion in Isolated Ileal, Proximal, and Mid-colonic Mucosa of WT Mice

HCO_3^- output rates ($J_{\text{HCO}_3^-}$) into the luminal bath were quantified in the isolated ileal as well as proximal and mid-colonic mucosa from $\text{TNF}^{+/+}$ mice. Ileal and mid-colonic $J_{\text{HCO}_3^-}$ was unexpectedly high in $\text{TNF}^{+/+}$ mucosa, whereas proximal colonic $J_{\text{HCO}_3^-}$ was low (Fig. 2A). The removal of Cl^- from the luminal bath resulted in a strong decrease in $J_{\text{HCO}_3^-}$ in the $\text{TNF}^{+/+}$ mucosa, indicative of a luminal $\text{Cl}^-/\text{HCO}_3^-$ exchange process as the major HCO_3^- exit pathway in the ileum and mid-colon. In the proximal colon, which is only 1–1.5 cm in length, $J_{\text{HCO}_3^-}$ was found to be very low in the $\text{TNF}^{+/+}$ mucosa, with no reduction by the removal of luminal Cl^- and a low forskolin-induced HCO_3^- secretory response ($J_{\text{HCO}_3^-}$). This part of the colon was therefore not further studied in the current project.

Basal and cAMP-elicited I_{sc} was not significantly different in the mucosa from the three segments (Fig. 2B), underlining the fact that it is predominantly mediated by Cl^- rather than HCO_3^- secretion in the murine ileocolon in Cl^- containing luminal bath conditions.

Reduced HCO_3^- Secretion in Chronically Inflamed Distal Ileum and Colon In Vitro

In $\text{TNF}^{+/ \text{ ARE}}$ ileal mucosa, basal $J_{\text{HCO}_3^-}$ was strongly diminished in comparison to $\text{TNF}^{+/+}$ (Fig. 3A, left and middle panel) in a Cl^- -dependent fashion, indicative of a defect in electroneutral $\text{Cl}^-/\text{HCO}_3^-$ exchange. In addition, the forskolin-induced $J_{\text{HCO}_3^-}$ as well as I_{sc} was also reduced in $\text{TNF}^{+/ \text{ ARE}}$ ileal mucosa, indicating a defect in electrogenic HCO_3^- secretion (Fig. 3A,B, right panel). Basal I_{sc} was increased in $\text{TNF}^{+/ \text{ ARE}}$ inflamed ileum compared to $\text{TNF}^{+/+}$ (Fig. 3B), but since basal I_{sc} is a sum signal from a multitude of apical and basolateral, as well as tight junctional transport processes, no interpretation of this finding was attempted.

In mid-colonic mucosa, luminal Cl^- -dependent $J_{\text{HCO}_3^-}$ was high in the $\text{TNF}^{+/+}$ mucosa, and strongly decreased in the $\text{TNF}^{+/ \text{ ARE}}$ mucosa. In contrast, $J_{\text{HCO}_3^-}$ was not significantly altered (Fig. 4A). Basal I_{sc} as well as I_{sc} in the $\text{TNF}^{+/ \text{ ARE}}$ mid-colonic mucosa were not significantly altered (Fig. 4B).

HCO_3^- Secretory Rates in $\text{TNF}^{+/ \text{ ARE}}$ Distal Ileum and Colon Were Reduced In Vivo

The distal ileum as well as the more proximal and more distal part of the colon (called proximal-mid- and mid-distal colon, because there is overlap of the perfused segments in the mid-colon region) of $\text{TNF}^{+/ \text{ ARE}}$ and $\text{TNF}^{+/+}$ mice were also studied in vivo. The distal ileum of $\text{TNF}^{+/+}$ mice displayed basal $J_{\text{HCO}_3^-}$ that were $\approx 2\text{--}3$ times higher than those observed in the duodenum in mice of the same genetic background,²⁰ and were significantly reduced in the ileum of $\text{TNF}^{+/ \text{ ARE}}$ mice (Fig. 5A). Removal of Cl^- from the perfusate reduced $J_{\text{HCO}_3^-}$ in $\text{TNF}^{+/ \text{ ARE}}$ and more so in $\text{TNF}^{+/+}$ ileum, subsequent stimulation by intraluminal forskolin elicited a secretory response that was significantly reduced in the

TNF^{+/-} ARE compared to the TNF^{+/+} ileum. Thus, the in vivo results corresponded qualitatively with the in vitro data from isolated ileal mucosa.

Colonic perfusion is technically challenging, because dilatation caused by fluid trapping may elicit secretory reflexes. The proximal-mid-colonic segment that was perfused in vivo is therefore slightly longer and slightly more distal than the one studied in the Ussing chamber in Figure 2. However, significant reduction of basal J_{HCO₃⁻} was seen in both the proximal-mid- and the mid-distal colon (Fig. 5B).

DRA, PAT-1, NHE3, and CFTR mRNA Expression, and DRA Immunohistochemistry in Chronically Inflamed Intestine

The defect in Cl⁻-dependent J_{HCO₃⁻} suggests a disturbance in apical Cl⁻/HCO₃⁻ exchange. Accordingly, a significant decrease in DRA as well as PAT-1 mRNA was found in inflamed ileum, in relation of each of three control genes (Fig. 6A). mRNA expression levels for a number of other genes implicated in ileal acid/base transport, including CFTR and NHE3, were not significantly decreased, except for carbonic anhydrase IV (CAIV), which was strongly downregulated (Supplementary Fig. 1). However, ileal HCO₃⁻ secretion was unaltered in CAIV-deficient mice (Supplementary Fig. 1).

Similar to the situation in the ileum, a strong decrease was observed for DRA mRNA in the mid-distal colonic mucosa (Fig. 6B), while levels of CFTR and NHE3 mRNA were not altered in relation to the control gene in mid-colonic mucosa (Fig. 6B). PAT-1 was not studied because it is not significantly expressed in the colon.

Immunolabeling confirmed the decreased expression of DRA in the colon of the TNF^{+/-} ARE mice (Fig. 6C). Specificity of the antibodies was confirmed by testing the respective segments in DRA^{-/-} mice (Supplementary Fig. 2). The results indicate that DRA mRNA expression is exquisitely sensitive to downregulation by proinflammatory cytokines.

Ileal and Colonic Fluid Absorption in TNF^{+/-} ARE and TNF^{+/+} Ileum and Colon In Vivo

DRA-deficiency is both related to defective HCO₃⁻ secretion as well as NaCl absorption. The TNF^{+/-} ARE mice do not develop severe diarrhea. We therefore studied ileal and mid-distal colonic fluid absorption in vivo. A marked reduction in forskolin-sensitive fluid absorption was seen in the distal ileum of TNF^{+/-} ARE in comparison to WT (Fig. 7A). In the mid-distal colon, fluid absorptive rates were not significantly different between TNF^{+/-} ARE and TNF^{+/+} mice, and the ENaC inhibitor amiloride reduced fluid absorption significantly more strongly in the TNF^{+/-} ARE than the TNF^{+/+} mid-distal colon of anesthetized mice (Fig. 7B), possibly suggesting partial compensation for more proximal fluid absorptive defects.

Spontaneous and Aldosterone-induced ENaC Activity in the Distal Colon of TNF^{+/-} ARE and TNF^{+/+} Mice

Since the well-preserved, and partly amiloride-sensitive mid-distal colonic fluid absorption in vivo suggested ENaC- as well as NHE-mediated salt absorption (which was surprising to us since ENaC dysfunction has been well demonstrated in colonic inflammation⁷), we investigated the amiloride-induced I_{sc} response in the distal colonic mucosa of TNF^{+/-} ARE

and TNF^{+/+} mice under standard and after 3 weeks low salt chow. Interestingly, the spontaneous ENaC current was even slightly higher in the TNF^{+/ARE} than TNF^{+/+} mice, and the induction of ENaC current after low salt diet was similar in TNF^{+/ARE} compared to TNF^{+/+} mice. ENaC subunit mRNA upregulation after low salt diet was not significantly different in TNF^{+/+} and TNF^{+/ARE} mice (Fig. 8). This suggested that the marked increase in proinflammatory cytokines and neutrophil infiltration (see Fig. 1A–C) per se is not sufficient to result in severe disturbances in ENaC function. Indeed, an enhancement glucocorticoid-induced ENaC expression by TNF- α has recently been demonstrated in vitro,²³ which may help explain these findings.

Discussion

Luminal HCO₃⁻ has been found essential for the release and proper function of intestinal mucus,²⁴ intestinal wound healing^{25,26} and intestinal electrolyte reabsorption.²⁷ Intraluminal pH has been also found to be abnormally low in a number of studies in the colon of patients with UC,²⁸ but the importance of this has so far been discussed predominantly in the context of antiinflammatory drug release.²⁸ In the pancreas, however, ductal injury reduced HCO₃⁻ secretion and enhances the risk for acute pancreatitis.²⁹ An inflammation-associated HCO₃⁻ secretory defect may, therefore, weaken the natural defenses necessary for the healing of mucosal damage, and restoration of luminal HCO₃⁻ may be a therapeutic goal. Therefore, this study was designed to get further insight into the mechanisms that are responsible for a reduction in HCO₃⁻ secretion, if any, in intestinal inflammation.

Murine ileocolonic mucosa displayed very high HCO₃⁻ secretory rates when compared with any other part of the murine GI tract. Even mildly inflamed murine ileocolonic mucosa displayed strongly reduced epithelial HCO₃⁻ secretory rates in vivo and in vitro even in the absence of overt diarrhea. A strong defect was found both for ileal and mid-distal colonic mucosa in vivo, the two areas with the highest HCO₃⁻ secretory rates in the murine intestinal tract, despite the fact that the ileum was the area of maximal inflammatory severity in this model.

The next task was to identify the molecular mechanisms responsible for reduced HCO₃⁻ output to the lumen. “HCO₃⁻ secretion” or “luminal alkalinization” is an extremely complex process, since HCO₃⁻ ions can be transported across luminal membrane either in exchange against another anion, can pass through anion conductance or anion-selective pores in the tight junction complexes, or can be generated from CO₂ that perfuses to the lumen. A differentiation between HCO₃⁻/anion exchange mechanisms and HCO₃⁻ conductance can be made by assessing the dependency of the movement of HCO₃⁻ to that of another anion into the opposite direction. Sundaram and West³⁰ have studied Cl⁻/HCO₃⁻ exchange rates in isolated ileal villus and crypt enterocytes from a rabbit infectious chronic colitis model and found significant decrease in the anion exchange activity in the villus cells of the inflamed ileum. The same was true for short chain fatty acid/HCO₃⁻ exchange.³¹ Zhang et al³² studied an acute “inflammation” model in mouse ileum, where anti-CD3 antibodies were injected to cause acute T-cell-mediated cytokine release, and within 3 hours after the

injection observed a shift from an electroneutral, Cl^- -dependent and DIDS-sensitive to an electrogenic, CFTR-dependent, glibenamide-sensitive type of HCO_3^- secretion. The molecular nature of the affected anion exchanger remained unresolved in these studies. However, Yang et al¹² found a dramatic decrease in DRA expression in the distal colon of patients with active UC, as well as in a rat and a mouse colitis model. Since the strong defect in basal HCO_3^- secretion both in the ileum and the mid-colon of the $\text{TNF}^{+/ \text{ARE}}$ mice was only seen in the presence of luminal Cl^- , a DRA dysfunction as the causative mechanism for the reduced HCO_3^- secretion was a reasonable assumption. Indeed, we observed decreased mRNA expression levels for both ileal $\text{Cl}^-/\text{HCO}_3^-$ exchangers, PAT-1 as well as DRA. However, PAT-1 knockout mice had no defect in ileal HCO_3^- secretion, ruling out an involvement in the inflammation-associated HCO_3^- secretory defect (Xiao F, Singh AK, unpubl. obs.). In the colon, where PAT-1 is only weakly expressed,³³ a significant difference in basal HCO_3^- was observed between $\text{TNF}^{+/ \text{ARE}}$ and $\text{TNF}^{+/+}$ mucosa, despite a histologically less severe inflammation. This was seen both in vivo and in vitro. Interestingly, DRA mRNA expression was strongly downregulated when compared to both epithelial-specific and nonspecific control genes, but also in comparison to other transporters like NHE3 and CFTR.

We were surprised by this strong DRA-dependent defect in colonic HCO_3^- secretion, because we had anticipated DRA to operate in parallel with NHE3, resulting in NaCl absorption and a balanced secretion of both HCO_3^- and H^+ .^{20,34} We therefore measured the fluid absorptive capacity of both the distal ileum and the mid-distal colon. While the ileal absorptive capacity was severely reduced, that of the mid-distal colon was relatively well maintained. This surprised us, because externally applied cytokines $\text{TNF-}\alpha$ or $\text{INF-}\gamma$ have been causally linked to downregulation of Na^+ absorptive transporters in cultured cells and isolated colonic mucosa.^{5,6} The cytokine levels for $\text{TNF-}\alpha$, $\text{INF-}\gamma$, and $\text{IL-1}\beta$ in the mid-distal colon of the $\text{TNF}^{+/ \text{ARE}}$ mice were higher in comparison to noninflamed mucosa than in the biopsies from IBD patients, in which such decreased Na^+ or fluid absorptive rates had been demonstrated,^{9,34} yet mid-distal colon fluid absorption was well maintained. We therefore studied ENaC activity and ENaC subunit mRNA expression in the distal colon of $\text{TNF}^{+/ \text{ARE}}$ and $\text{TNF}^{+/+}$ mice under control conditions and after 3 weeks of low sodium diet. ENaC activity was normal in $\text{TNF}^{+/ \text{ARE}}$ distal colon and could be further induced by low sodium diet, and ENaC subunit mRNA was not different between $\text{TNF}^{+/ \text{ARE}}$ and $\text{TNF}^{+/+}$ mucosa, demonstrating intact aldosterone-mediated upregulation of ENaC subunit expression despite histological and molecular biological evidence of inflammation. This demonstrates an exquisite sensitivity of DRA expression to inflammatory cytokines, not shared by other major colonic epithelial ion transporters such as NHE3, ENaC, or CFTR. This sensitivity may possibly be related to the observed downregulation of DRA promoter activity by $\text{INF-}\gamma$.³⁵

The preserved ENaC function, as well as ENaC subunit regulation, may be explained by the recent observations by Bergann et al,²³ who found that $\text{TNF-}\alpha$ may enhance glucocorticoid-induced ENaC expression via stabilization of glucocorticoid receptors. We assumed the increased amiloride-sensitivity of mid-distal colonic fluid absorption in $\text{TNF}^{+/ \text{ARE}}$ mice to

possibly reflect increased aldosterone levels due to proximal defects in fluid absorption, but increased levels of stress hormones are also feasible in the arthritic mice.

The defect in forskolin-induced, but Cl^- independent $\text{J}_{\text{HCO}_3^-}$ in the $\text{TNF}^{+/ \Delta \text{RE}}$ ileum, combined with a reduction of I_{sc} response, reminds one of a CFTR-mediated defect.¹⁶ However, CFTR mRNA expression was not downregulated in the ileum of $\text{TNF}^{+/ \Delta \text{RE}}$ mice. Likewise, this disturbance was not seen in the mid-colonic mucosa despite similar degrees of DRA downregulation. Further explorations of potential defects in the HCO_3^- uptake or supply pathways in inflamed ileum were essentially negative. While we found a downregulation of CAIV mRNA expression in inflamed ileum, CAIV-deficient mice displayed no decrease in basal or agonist-induced HCO_3^- secretion. Upregulation of other CA isoforms may compensate for its function, or it may not be involved in ileal HCO_3^- secretion. Thus, we assume that disturbances in the signaling pathway for regulating the CFTR HCO_3^- conductivity during inflammation, or the overall villus plumping with reduction of epithelial surface area, may be explanations for the observed defect in forskolin-induced Cl^- -independent HCO_3^- secretory response in $\text{TNF}^{+/ \Delta \text{RE}}$ ileum.

Lastly, what may be the pathophysiologic relevance of our findings? Of course, all inflammatory mouse models have caveats when used as models for human IBD. Our mouse model resembles Crohn's disease (CD) rather than UC in humans, because of the strongest manifestation in the ileum and because of the strong expression of Th1 cytokines. The relative increase of TH1 cytokine mRNA expression in comparison to noninflamed control tissue is similar or higher in this mouse model than in any other model that we have studied (IL-10 KO, transfer colitis, DSS colitis) as well as in CD and UC patient biopsies, even in the distal colon, which only shows mild inflammation in this mouse model. So we believe that it is a good model to assess the effects of elevated Th1 cytokine levels in the range that actually occur in inflamed IBD intestine.^{9,34} Obviously, it cannot mimic human disease, because these mice develop no fissuring disease, no granuloma development, and their course is nonremitting. However, similar to many CD patients, these mice have no overt diarrhea. Therefore, our study helps to understand that the absence of diarrhea need not indicate the absence of ion transport defects in inflamed colon, and that other pathophysiological aspects of deranged transport function need to be considered. The relevance of a defect in HCO_3^- secretion in colonic mucosa may be manifold: The role of HCO_3^- for mucosal protection against low luminal pH has been extensively studied in the upper GI tract.^{25,26,36,37} Drugs that are weak acids permeate and damage the epithelial cells more at lower luminal pH than in an alkaline environment.³⁸⁻⁴⁰ Epithelial wound healing requires an alkaline surface pH both in the upper GI tract and in the colon.^{25,26,41} Alkaline phosphatase ectoenzymatic activity is highly pH-sensitive and has recently been implicated in mucosal defense.^{42,43} Intact HCO_3^- secretion has been shown essential for mucus secretion in intestine, airways, and reproductive tract.^{24,44,45} An intact mucus layer has recently been shown to be essential for the prevention of bacteria to attach to the colonic mucosa and elicit an inflammatory response.⁴⁶ Our mouse model cannot be used to address the potential consequences of such low HCO_3^- output to mucosal health, but nevertheless poses new questions for future research. Such research may even help to explain why in CD

patients the inflammation initially is restricted to the ileum but often also involves the distal colon at later stages of the disease.

In summary, our study data show that in a mouse model for mild ileocolonic inflammation, the anion exchanger DRA (Slc26a3) mRNA and protein expression is exquisitely sensitive to inflammation. The pathophysiological correlate need not be overt diarrhea, but may be low HCO_3^- output, leading to low surface pH in the mucus layer,⁴⁷ and likely alterations in colonic absorption, gut flora, and barrier properties. Studies of the pathophysiological consequence of defective luminal alkalinization in the ileocolonic mucosa seem warranted.

Acknowledgments

We thank Regina Engelhardt, Brigitte Rausch, and Natascha Cirpka for help with animal breeding and genotyping.

Supported by the Deutsche Forschungsgemeinschaft grants SFB621-C9, and Se460/13-4 (to U.S.) SFB621-C10 (to O.B.), and the DFG Chinese-German exchange grant DFG 446 CHV 113/268/0-1 (to U.S. and J.Z.).

References

1. Surawicz CM. Mechanisms of diarrhea. *Curr Gastroenterol Rep.* 2010; 12:236–241. [PubMed: 20532705]
2. Schmitz H, Barmeyer C, Fromm M, et al. Altered tight junction structure contributes to the impaired epithelial barrier function in ulcerative colitis. *Gastroenterology.* 1999; 116:301–309. [PubMed: 9922310]
3. Seidler U, Lenzen H, Cinar A, et al. Molecular mechanisms of disturbed electrolyte transport in intestinal inflammation. *Ann N Y Acad Sci.* 2006; 1072:262–275. [PubMed: 17057206]
4. Greig ER, Mathialahan T, Boot-Handford RP, et al. Molecular and functional studies of electrogenic Na^+ transport in the distal colon and rectum of young and elderly subjects. *Gut.* 2003; 52:1607–1615. [PubMed: 14570731]
5. Amin MR, Malakooti J, Sandoval R, et al. IFN-gamma and TNF-alpha regulate human NHE3 gene expression by modulating the Sp family transcription factors in human intestinal epithelial cell line C2BBE1. *Am J Physiol Cell Physiol.* 2006; 291:C887–896. [PubMed: 16760259]
6. Amin MR, Orenuga T, Tyagi S, et al. Tumor necrosis factor-alpha represses the expression of NHE2 through NF-kappaB activation in intestinal epithelial cell model, C2BBE1. *Inflamm Bowel Dis.* 2011; 17:720–731. [PubMed: 20722069]
7. Amasheh S, Barmeyer C, Koch CS, et al. Cytokine-dependent transcriptional down-regulation of epithelial sodium channel in ulcerative colitis. *Gastroenterology.* 2004; 126:1711–1720. [PubMed: 15188166]
8. Clayburgh DR, Musch MW, Leitges M, et al. Coordinated epithelial NHE3 inhibition and barrier dysfunction are required for TNF-mediated diarrhea in vivo. *J Clin Invest.* 2006; 116:2682–2694. [PubMed: 17016558]
9. Farkas K, Yeruva S, Rakoncay Z, et al. New therapeutic targets in ulcerative colitis: The importance of ion transporters in the human colon. *Inflamm Bowel Dis.* 2011; 17:884–898. [PubMed: 20722063]
10. Walker NM, Simpson JE, Brazill JM, et al. Role of down-regulated in adenoma anion exchanger in HCO_3^- secretion across murine duodenum. *Gastroenterology.* 2009; 136:893–901. [PubMed: 19121635]
11. Walker NM, Simpson JE, Yen PF, et al. Down-regulated in adenoma $\text{Cl}^-/\text{HCO}_3^-$ exchanger couples with Na^+/H^+ exchanger 3 for NaCl absorption in murine small intestine. *Gastroenterology.* 2008; 135:1645–1653 e3. [PubMed: 18930060]
12. Yang H, Jiang W, Furth EE, et al. Intestinal inflammation reduces expression of DRA, a transporter responsible for congenital chloride diarrhea. *Am J Physiol.* 1998; 275:G1445–1453. [PubMed: 9843783]

13. Lohi H, Makela S, Pulkkinen K, et al. Upregulation of CFTR expression but not SLC26A3 and SLC9A3 in ulcerative colitis. *Am J Physiol Gastrointest Liver Physiol.* 2002; 283:G567–575. [PubMed: 12181169]
14. Kontoyiannis D, Pasparakis M, Pizarro TT, et al. Impaired on/off regulation of TNF biosynthesis in mice lacking TNF AU-rich elements: implications for joint and gut-associated immunopathologies. *Immunity.* 1999; 10:387–398. [PubMed: 10204494]
15. Bleich A, Mahler M, Most C, et al. Refined histopathologic scoring system improves power to detect colitis QTL in mice. *Mamm Genome.* 2004; 15:865–871. [PubMed: 15672590]
16. Tuo B, Riederer B, Wang Z, et al. Involvement of the anion exchanger SLC26A6 in prostaglandin E2- but not forskolin-stimulated duodenal HCO₃⁻ secretion. *Gastroenterology.* 2006; 130:349–358. [PubMed: 16472591]
17. Singh AK, Sjoblom M, Zheng W, et al. CFTR and its key role in in vivo resting and luminal acid-induced duodenal HCO₃⁻ secretion. *Acta Physiol (Oxf).* 2008; 193:357–365. [PubMed: 18363901]
18. Singh AK, Amlal H, Haas PJ, et al. Fructose-induced hypertension: essential role of chloride and fructose absorbing transporters PAT1 and Glut5. *Kidney Int.* 2008; 74:438–447. [PubMed: 18496516]
19. Sjoblom M, Singh AK, Zheng W, et al. Duodenal acidity “sensing” but not epithelial HCO₃⁻ supply is critically dependent on carbonic anhydrase II expression. *Proc Natl Acad Sci USA.* 2009; 106:13094–13099. [PubMed: 19622732]
20. Singh AK, Riederer B, Chen M, et al. The switch of intestinal Slc26 exchangers from anion absorptive to HCO₃⁻ secretory mode is dependent on CFTR anion channel function. *Am J Physiol Cell Physiol.* 2010; 298:C1057–1065. [PubMed: 20164375]
21. Broere N, Chen M, Cinar A, et al. Defective jejunal and colonic salt absorption and altered Na⁽⁺⁾/H⁽⁺⁾ exchanger 3 (NHE3) activity in NHE regulatory factor 1 (NHERF1) adaptor protein-deficient mice. *Pflugers Arch.* 2009; 457:1079–1091. [PubMed: 18758809]
22. Gill RK, Borthakur A, Hodges K, et al. Mechanism underlying inhibition of intestinal apical Cl⁻/OH⁻ exchange following infection with enteropathogenic *E. coli*. *J Clin Invest.* 2007; 117:428–437. [PubMed: 17256057]
23. Bergann T, Zeissig S, Fromm A, et al. Glucocorticoids and tumor necrosis factor- α synergize to induce absorption by the epithelial sodium channel in the colon. *Gastroenterology.* 2009; 136:933–942. [PubMed: 19185581]
24. Garcia MA, Yang N, Quinton PM. Normal mouse intestinal mucus release requires cystic fibrosis transmembrane regulator-dependent bicarbonate secretion. *J Clin Invest.* 2009; 119:2613–2622. [PubMed: 19726884]
25. Baumann M, Arlt G, Winkeltau G, et al. Significance of pancreatic and duodenal secretions for the protection of gastrointestinal anastomoses following stomach resection—an animal experiment study. *Lan-genbecks Arch Chir.* 1988; 373:109–113.
26. Feil W, Klimesch S, Karner P, et al. Importance of an alkaline microenvironment for rapid restitution of the rabbit duodenal mucosa in vitro. *Gastroenterology.* 1989; 97:112–122. [PubMed: 2721864]
27. Binder HJ, Rajendran V, Sadasivan V, et al. Bicarbonate secretion: a neglected aspect of colonic ion transport. *J Clin Gastroenterol.* 2005; 39:S53–58. [PubMed: 15758660]
28. Nugent SG, Kumar D, Rampton DS, et al. Intestinal luminal pH in inflammatory bowel disease: possible determinants and implications for therapy with aminosaliculates and other drugs. *Gut.* 2001; 48:571–577. [PubMed: 11247905]
29. Hegyi P, Rakonczay Z. Insufficiency of electrolyte and fluid secretion by pancreatic ductal cells leads to increased patient risk for pancreatitis. *Am J Gastroenterol.* 2010; 105:2119–2120.
30. Sundaram U, West AB. Effect of chronic inflammation on electrolyte transport in rabbit ileal villus and crypt cells. *Am J Physiol.* 1997; 272:G732–741. [PubMed: 9142903]
31. Manokas T, Fromkes JJ, Sundaram U. Effect of chronic inflammation on ileal short-chain fatty acid/bicarbonate exchange. *Am J Physiol Gastrointest Liver Physiol.* 2000; 278:G585–590. [PubMed: 10762613]

32. Zhang H, Ameen N, Melvin JE, et al. Acute inflammation alters bicarbonate transport in mouse ileum. *J Physiol*. 2007; 581:1221–1233. [PubMed: 17395634]
33. Wang Z, Petrovic S, Mann E, et al. Identification of an apical Cl⁻/HCO₃⁻ exchanger in the small intestine. *Am J Physiol Gastrointest Liver Physiol*. 2002; 282:G573–579. [PubMed: 11842009]
34. Yeruva S, Farkas K, Hubricht J, et al. Preserved Na⁽⁺⁾/H⁽⁺⁾ exchanger isoform 3 expression and localization, but decreased NHE3 function indicate regulatory sodium transport defect in ulcerative colitis. *Inflamm Bowel Dis*. 2010; 16:1149–1161. [PubMed: 20027604]
35. Saksena S, Singla A, Goyal S, et al. Mechanisms of transcriptional modulation of the human anion exchanger SLC26A3 gene expression by IFN-gamma. *Am J Physiol Gastrointest Liver Physiol*. 2010; 298:G159–166. [PubMed: 19940027]
36. Ross IN, Turnberg LA. Studies of the ‘mucus-bicarbonate’ barrier on rat fundic mucosa: the effects of luminal pH and a stable prostaglandin analogue. *Gut*. 1983; 24:1030–1033. [PubMed: 6629112]
37. Shorrock CJ, Rees WD. Overview of gastroduodenal mucosal protection. *Am J Med*. 1988; 84:25–34. [PubMed: 3279766]
38. Ashley SW, Soybel DI, Moore CD, et al. Effects of aspirin and acetic acid on intracellular pH in necturus gastric mucosa. *Am J Surg*. 1989; 157:66–73. [PubMed: 2910129]
39. Nuernberg B, Szelenyi I, Schneider HT, et al. Diflunisal disposition. Role of gastric absorption in the development of mucosal damage and anti-inflammatory potency in rodents. *Drug Metab Dispos*. 1990; 18:937–942. [PubMed: 1981540]
40. Soybel DI, Davis MB, West AB. Effects of aspirin on pathways of ion permeation in Necturus antrum: role of nutrient HCO₃⁻. *Gastroenterology*. 1992; 103:1475–1485. [PubMed: 1330800]
41. Semble EL, Wu WC. Prostaglandins in the gut and their relationship to non-steroidal anti-inflammatory drugs. *Baillieres Clin Rheumatol*. 1989; 3:247–269. [PubMed: 2670254]
42. Bol-Schoenmakers M, Fiechter D, Raaben W, et al. Intestinal alkaline phosphatase contributes to the reduction of severe intestinal epithelial damage. *Eur J Pharmacol*. 2010; 633:71–77. [PubMed: 20132812]
43. Lalles JP. Intestinal alkaline phosphatase: multiple biological roles in maintenance of intestinal homeostasis and modulation by diet. *Nutr Rev*. 2010; 68:323–332. [PubMed: 20536777]
44. Chen EY, Yang N, Quinton PM, et al. A new role for bicarbonate in mucus formation. *Am J Physiol Lung Cell Mol Physiol*. 2010; 299:L542–549. [PubMed: 20693315]
45. Muchekeh RW, Quinton PM. A new role for bicarbonate secretion in cervico-uterine mucus release. *J Physiol*. 2010; 588:2329–2342. [PubMed: 20478977]
46. Johansson ME, Gustafsson JK, Sjöberg KE, et al. Bacteria penetrate the inner mucus layer before inflammation in the dextran sulfate colitis model. *PLoS One*. 2010; 5:e12238. [PubMed: 20805871]
47. Talbot C, Lytle C. Segregation of Na/H exchanger-3 and Cl⁻/HCO₃⁻ exchanger SLC26A3 (DRA) in rodent cecum and colon. *Am J Physiol Gastrointest Liver Physiol*. 2010; 299:G358–367. [PubMed: 20466943]

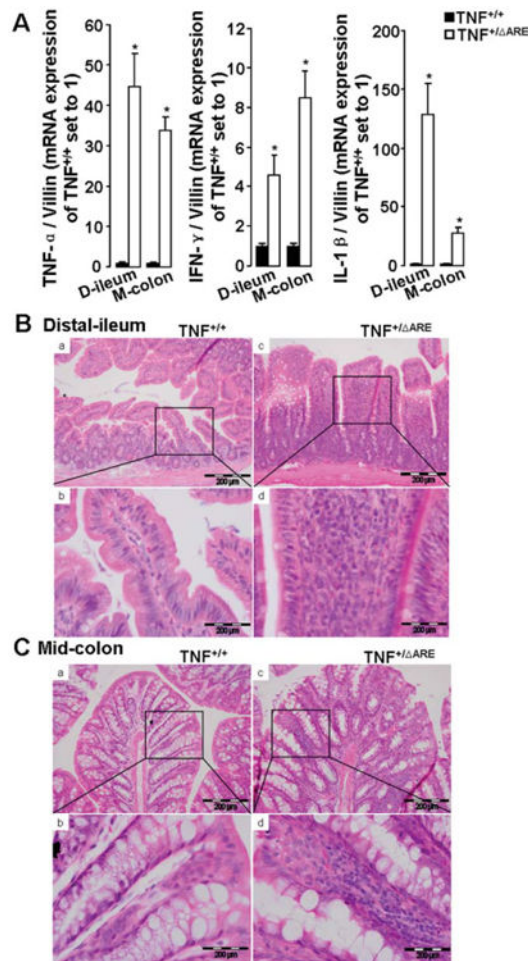


Figure 1. Manifestation of chronic inflammation in TNF^{+/ΔARE} mice distal-ileum and mid-colon. (A) Increase of mRNA expression for the proinflammatory cytokines TNF- α (left panel), IFN- γ (middle panel), and IL-1 β (right panel) in the distal ileum and the mid-colon of TNF^{+/ΔARE} (□) mice in relation to the TNF^{+/+} controls (■). mRNA expression in the TNF^{+/+} was set to 1. Villin was used as control gene. * $P < 0.05$ versus TNF^{+/+}. $n = 4$. (B) Distal ileal histology, with marked villus blunting and inflammatory cell infiltration in TNF^{+/ΔARE} mice (c,d) compared to TNF^{+/+} (a,b). (C) Mid-colonic histology, with submucosal inflammatory cell infiltration in TNF^{+/ΔARE} mice (c,d) compared to TNF^{+/+} (a,b) and slight crypt and goblet cell hypertrophy. Scale bars = 200 μ m.

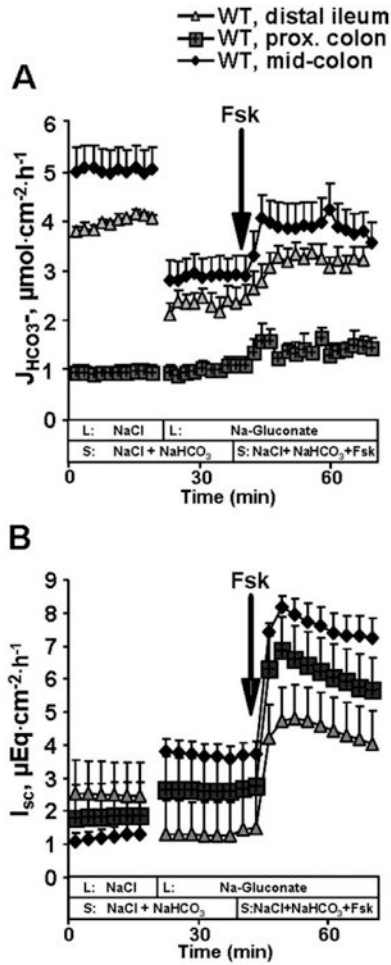


Figure 2.

$J_{\text{HCO}_3^-}$ and I_{sc} in different segments of murine ileocolon. (A) Time course of $J_{\text{HCO}_3^-}$ and (B) I_{sc} in the presence and absence of luminal Cl^- and after forskolin stimulation across $\text{TNF}^{+/+}$ distal ileal, proximal, and mid-colonic mucosa. (A) Ileal and mid-colonic mucosa display high basal $J_{\text{HCO}_3^-}$, which were strongly reduced by removal of Cl^- from the luminal perfusate and therefore to a large part mediated by $\text{Cl}^-/\text{HCO}_3^-$ exchange. In the proximal colon (first 1–1.5 cm of colon), basal $J_{\text{HCO}_3^-}$ was low and Cl^- independent. (B) No significant differences in basal and Fsk-stimulated I_{sc} (I_{sc}) among these segments of the intestine. The arrows indicate the addition of forskolin (Fsk, 10 μM) to the serosal bath. $n = 5-9$.

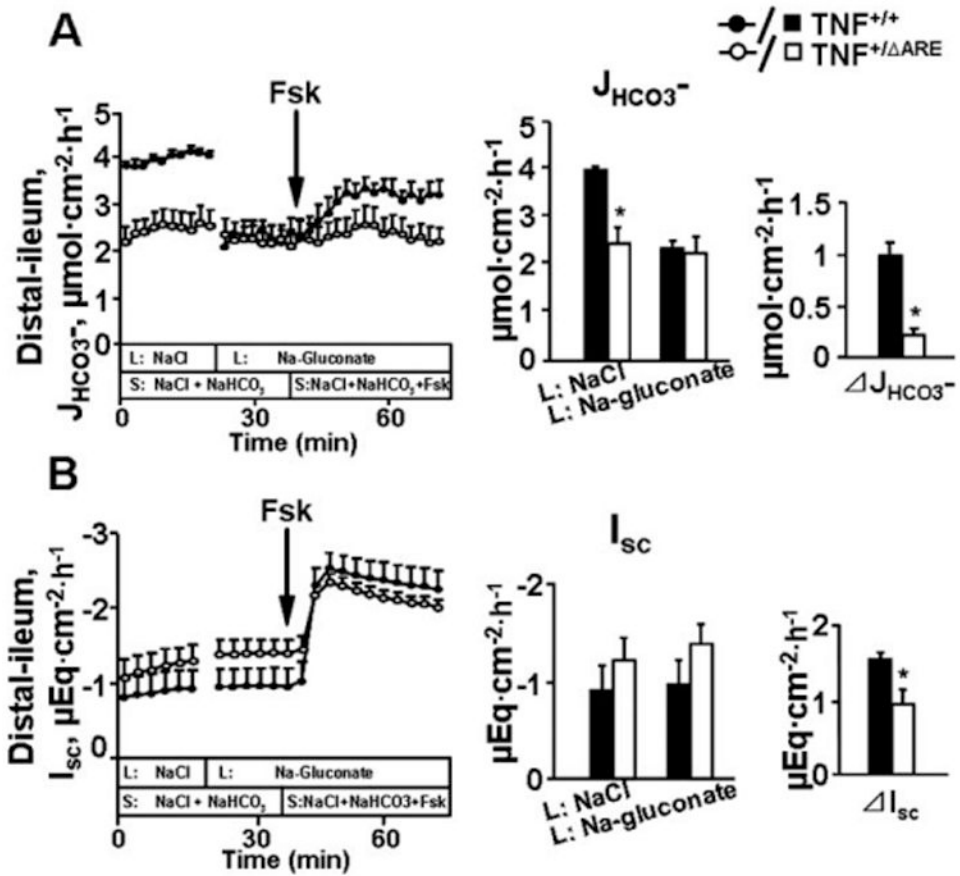


Figure 3.

Basal and forskolin-stimulated $J_{\text{HCO}_3^-}$ and I_{sc} across TNF^{+/ Δ ARE} and TNF^{+/+} littermate distal ileal mucosa. (A) $J_{\text{HCO}_3^-}$ was assessed in the presence and absence of luminal Cl^- , as well as after stimulation with forskolin (10^{-5}M), in TNF^{+/ Δ ARE} (□) and TNF^{+/+} (■) distal ileal mucosa. Left panel: Time course. Middle panel: $J_{\text{HCO}_3^-}$ in the presence (NaCl) and absence (Na-Gluconate) of Cl^- in the luminal bath. Right panel: forskolin-stimulated $J_{\text{HCO}_3^-}$. (B) Time course (left panel), basal I_{sc} in the presence and absence of luminal Cl^- (middle panel), and forskolin-stimulated I_{sc} (I_{sc} , right panel) across TNF^{+/ Δ ARE} (□) and TNF^{+/+} (■) distal ileal mucosa. * $P < 0.05$ versus TNF^{+/+}. $n = 7-8$.

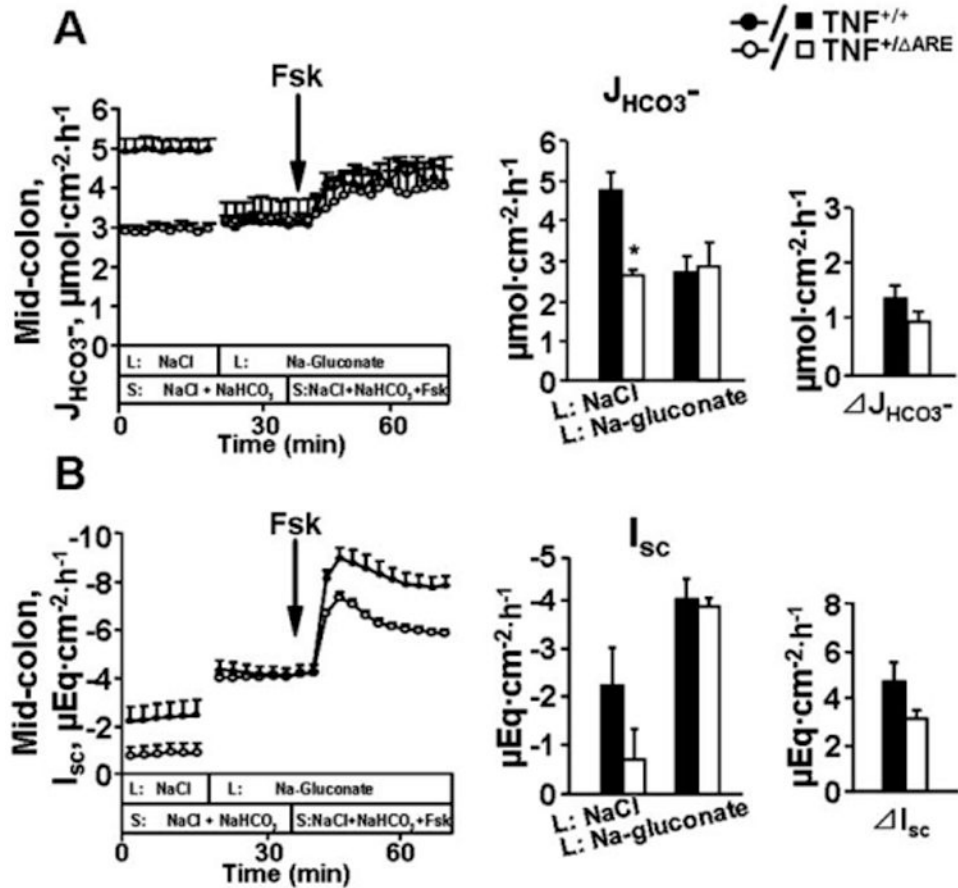


Figure 4.

Basal and forskolin-stimulated $J_{\text{HCO}_3^-}$ and I_{sc} across TNF^{+/ΔARE} and TNF^{+/+} mid-colonic mucosa. (A) $J_{\text{HCO}_3^-}$ was assessed in the presence and absence of luminal Cl^- , as well as after stimulation with forskolin (10^{-5}M), in TNF^{+/ΔARE} (□) and TNF^{+/+} (■) mid-colonic mucosa. Left panel: Time course. Middle panel: $J_{\text{HCO}_3^-}$ in the presence (NaCl) and absence (Na-Gluconate) of Cl^- in the luminal bath. Right panel: forskolin stimulated $J_{\text{HCO}_3^-}$. (B) Time course (left panel), basal I_{sc} in the presence and absence of luminal Cl^- (middle panel), and I_{sc} (right panel) in TNF^{+/ΔARE} (□) and TNF^{+/+} (■) mid-colonic mucosa. * $P < 0.05$ versus TNF^{+/+}. $n = 5$.

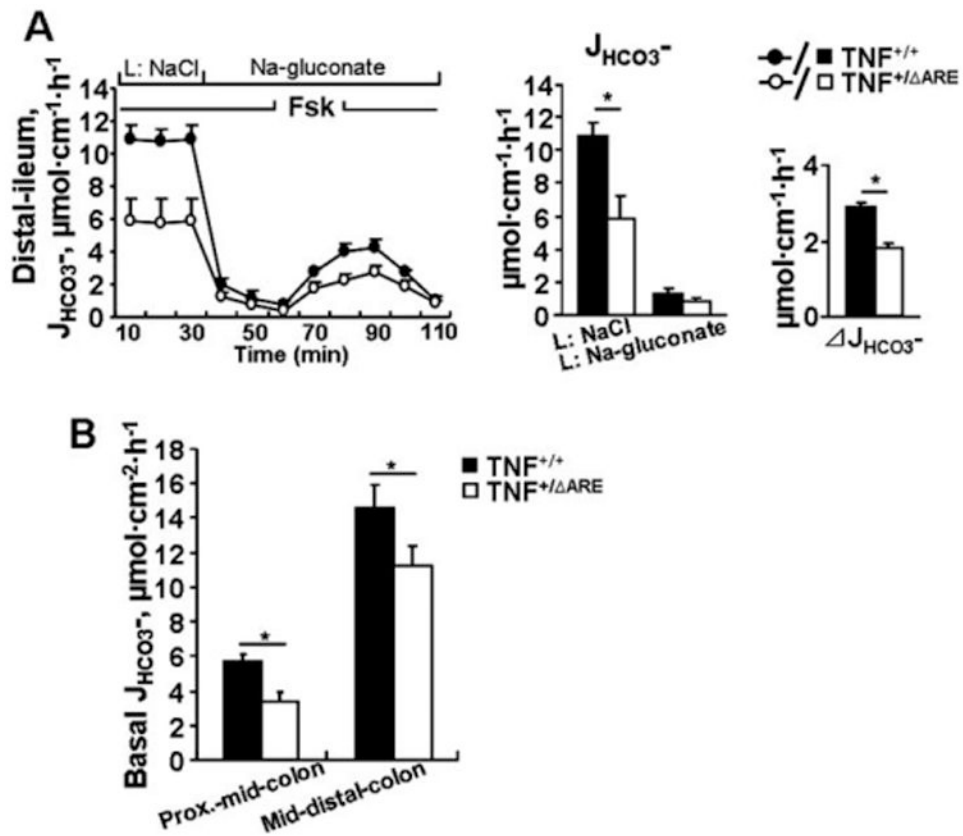


Figure 5.

$J_{\text{HCO}_3^-}$ in lumenally perfused distal ileum, proximal-mid, and mid-distal colon in anesthetized $\text{TNF}^{+/\Delta\text{ARE}}$ and $\text{TNF}^{+/+}$ mice. (A) Time course (left panel), basal $J_{\text{HCO}_3^-}$ in the presence and absence of luminal Cl^- (middle panel) and forskolin-stimulated $J_{\text{HCO}_3^-}$ ($J_{\text{HCO}_3^-}$, right panel) in perfused distal ileum of $\text{TNF}^{+/\Delta\text{ARE}}$ (□) and $\text{TNF}^{+/+}$ (■) mice. Both the basal $J_{\text{HCO}_3^-}$ (middle panel) as well as the forskolin-induced $J_{\text{HCO}_3^-}$ (right panel) are significantly reduced in $\text{TNF}^{+/\Delta\text{ARE}}$ ileum. (B) In inflamed proximal-mid (left panel) and mid-distal (right panel) colon, basal $J_{\text{HCO}_3^-}$ are significantly decreased in $\text{TNF}^{+/\Delta\text{ARE}}$ (□) compared to $\text{TNF}^{+/+}$ (■) mice in vivo. * $P < 0.05$ versus $\text{TNF}^{+/+}$. $n = 3-5$.

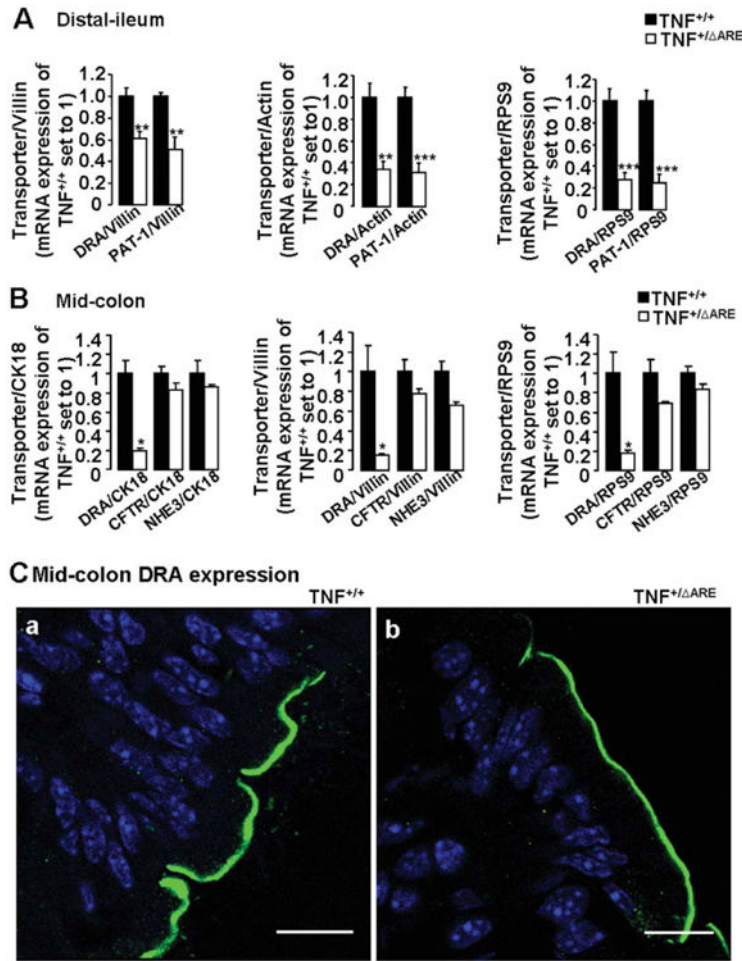


Figure 6. Significant decrease of DRA expression in the inflamed ileal and colonic mucosa. (A) mRNA expression for DRA and PAT-1 in the distal ileum of TNF^{+/-ΔARE} (□) was significantly decreased compared to TNF^{+/+} (■) ileum. The mRNA expression levels in the TNF^{+/+} ileum was set to 1. The qPCR was performed in both groups against villin (left panel), actin (middle panel), and RPS9 (right panel) as control genes. ***P* < 0.01, ****P* < 0.001 versus TNF^{+/+} mice. *n* = 4. (B) mRNA expression for DRA, CFTR, and NHE3 in the mid-colon of TNF^{+/-ΔARE} (□) compared to TNF^{+/+} (■) mid-colon. The qPCR was performed in both groups against cytokeratin 18 (left panel), villin (middle panel), and RPS9 (right panel) as control genes. **P* < 0.05 versus TNF^{+/+} mice. *n* = 4. (C) Immunofluorescence of DRA (green) in TNF^{+/-ΔARE} and TNF^{+/+} mice mid-colon. DRA fluorescence is decreased in the apical membrane of colonic enterocytes of TNF^{+/-ΔARE} (b) compared to TNF^{+/+} (a). Scale bars = 10 μm. A representative of three different experiments is shown.

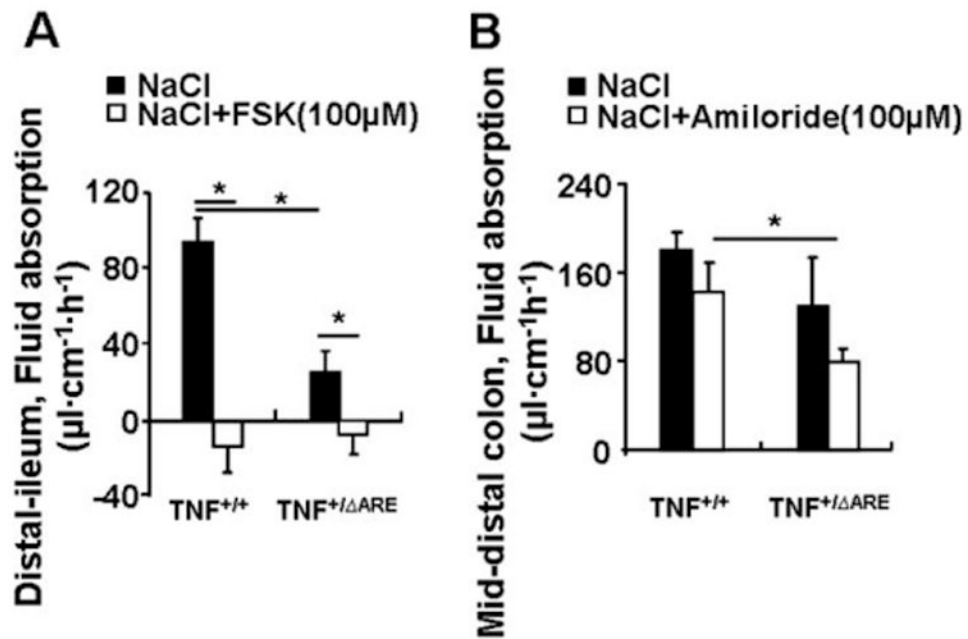


Figure 7.

Fluid absorption in the distal ileum and mid-distal colon of anesthetized $\text{TNF}^{+/\Delta\text{ARE}}$ and $\text{TNF}^{+/+}$ mice. (A) Fluid absorptive rates were strongly decreased in distal ileum of anesthetized $\text{TNF}^{+/\Delta\text{ARE}}$ compared to $\text{TNF}^{+/+}$ mice, and the fluid secretory response was also strongly reduced. $*P < 0.05$. $n = 5$. (B) In contrast, fluid absorptive rates in the mid-distal colon of $\text{TNF}^{+/\Delta\text{ARE}}$ mice were not significantly reduced compared to $\text{TNF}^{+/+}$ mice, and the ENaC inhibitor amiloride had even a slightly stronger inhibitory effect in the $\text{TNF}^{+/\Delta\text{ARE}}$ colon, indicative of intact ENaC function. $*P < 0.05$. $n = 4$.

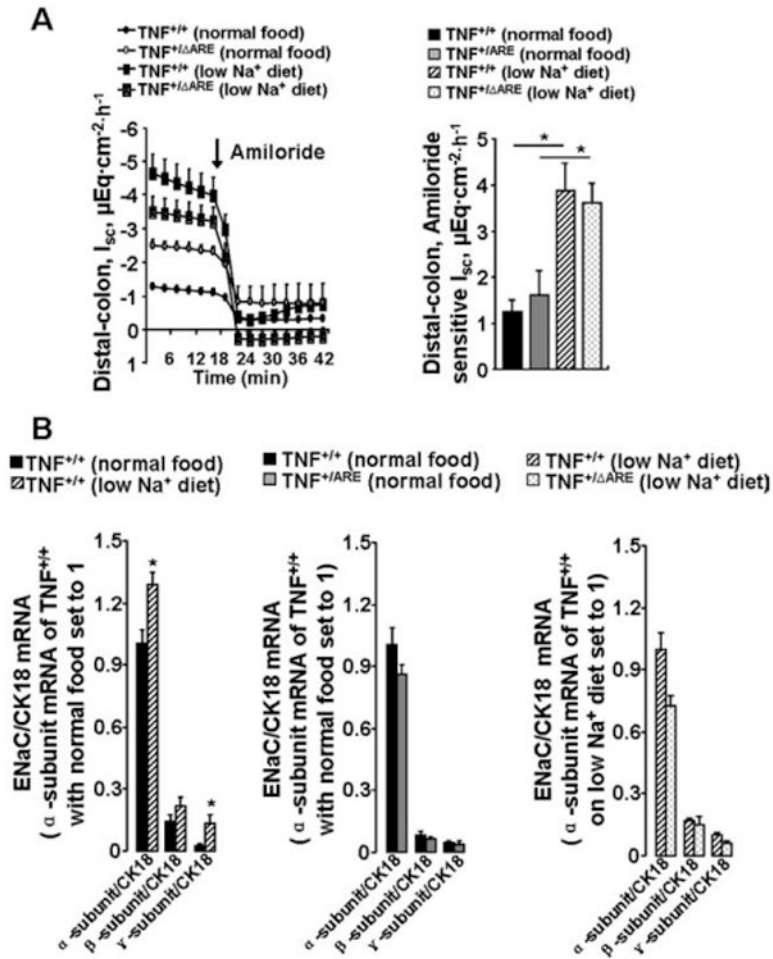


Figure 8.

Intact ENaC activity and normal ENaC mRNA expression in $\text{TNF}^{+/ARE}$ mice distal colon. (A) Left panel shows time course of amiloride-sensitive I_{sc} in distal colonic mucosa of $\text{TNF}^{+/ARE}$ and $\text{TNF}^{+/+}$ mice that were either fed with normal or low salt chow. Right panel: Differences in I_{sc} were measured before and after apical addition of amiloride ($10 \mu\text{M}$), and the amiloride-sensitive I_{sc} is displayed. $*P < 0.05$ versus normal food groups. $n = 4$. (B) ENaC subunit mRNA expression in the distal colon. Left panel shows mRNA expression of ENaC α , β , and γ subunit in distal colon of $\text{TNF}^{+/+}$ mice on either normal or after 3 weeks of low Na^+ diet, demonstrating upregulation of α and γ subunits. Middle panel: No significant difference in ENaC subunit expression was observed in $\text{TNF}^{+/ARE}$ and $\text{TNF}^{+/+}$ distal colon mice under standard chow. Right panel: After 3 weeks of low Na^+ diet, ENaC subunit expression was not significantly different in $\text{TNF}^{+/ARE}$ and $\text{TNF}^{+/+}$ distal colon, indicating intact stimulation of ENaC by salt restriction. In (B), the relative mRNA expression of the α -subunit in the $\text{TNF}^{+/+}$ colon was set to 1. Expression of ENaC subunits was standardized to that of the epithelial marker cytochrome 18. $*P < 0.05$ versus $\text{TNF}^{+/+}$. $n = 3-6$.